ORIGINAL PAPER

Failure Process of Rock Strata Due to Multi-seam Coal Mining: Insights from Physical Modelling

Yan Qin[1] · Nengxiong Xu[1] · Zhongjian Zhang[1] · Bin Zhang[1]

Abstract

With an increasing number of multi-seam mining projects, the problem of strata movement caused by multi-seam mining has attracted increasing attention. Previous studies have shown that the rock failure mechanism for multi-seam mining is obviously different from single-seam mining. When a lower coal seam is being mined, two issues are apparent: the activation that the upper goaf will suffer and the difference in the break mechanism of the stratum between single-seam and multi-seam mining. The research regarding these two issues is still inadequate. In this paper, a physical model experiment was used to simulate the full longwall mining process of multiple seams. Then, the failure mechanics of the stratum and the influence of mining the lower coal seam on the activation of the upper goaf are discussed under the condition that the upper coal seam has been fully mined. The results show that a part of the fracture zone that formed by mining the upper coal seam will be converted into a caving zone when the lower coal seam is mined. In multi-seam mining, the cracks in the overlying fractured rock mass will widen and propagate upward. During the process of mining the lower coal seam, the interburden rock mass presents a typical plate bending failure, and the break location is greatly affected by the distribution of the periodic weighting in the upper coal seam mining. Multi-seam mining will cause the surface subsidence trough produced by upper coal mining to move towards the end of the mining panel. The mechanism of rock stratum movement revealed by the test has a certain practical guidance for the control of roof pressure in multi-seam mining and the subsidence of surface.

Keywords Multi-seam mining · Full longwall mining · Failure process · Physical modelling

1 Introduction

In many countries, coal resources often exist as multiple coal seams. As the mining depth of coal resources increases, multi-seam mining will be faced by most mining areas. Previous studies have shown that multi-seam mining will cause more severe stress concentrations and more complicated surface subsidence than single-seam mining (Adhikary et al. 2015; Ma and Zhu 1984; Ren et al. 2014; Ma and Hu 2013; Ying-ke et al. 2011; Ghabraie et al. 2017a, b; Salmi et al. 2017). However, the strata movement mechanism caused by multi-seam mining have not been fully developed (Ghabraie et al. 2015). Therefore, the influence of strata movement caused by multi-seam mining on engineering stability has

attracted increasing attention from scholars (Tulu et al. 2016; Porathur et al. 2014; Suchowerska et al. 2012).

Similar to the research method of strata movement in single-seam mining, many scholars mainly use numerical simulations and physical model experiments to study strata movement in multi-seam mining (Helm et al. 2013; Miao et al. 2011; Salmi et al. 2017; Tang et al. 1998; Wang et al. 2017; Suchowerska et al. 2012).

On the one hand, some scholars have used numerical simulations to study the fracture propagation characteristics and stress distribution of the rock mass in multi-seam mining. Wei et al. (2011) used the finite element method (FEM) to study multi-seam mining, and the results showed that close distance multi-seam mining can lead to the propagation of old fissures and an increased height-increment in the fracture zone. Wang et al. (2012) found that the ratio of the fissure height to the mining thickness decreased with multi-seam mining. Liu et al. (2015) used the finite difference method (FDM) to study the developmental height of water conducting fissures in longwall mining of shallow buried

✉ Nengxiong Xu
xunengxiong@cugb.edu.cn

1   School of Engineering and Technology, China University of Geosciences (Beijing), Xueyuan Road 29, Beijing 100083, PR China

coal seams, and they indicated that the height of the fissures increases as the mining width and thickness increase, but it does not increase after reaching a certain height. Zhang et al. (2013) used the FDM to study the variation in stress in deep multi-seam mining. It is believed that the stress concentration caused by multi-seam mining mainly comes from the adjustment of the horizontal stress and the destruction of the interburden. Suchowerska et al. (2013) used FEM to study the effects of the abutment angle, overburden depth, pillar width, and anisotropic behaviour of the rock mass on the morphology and distribution of the vertical stress. Zhu and Tu (2017) used FDM to determine that the stress concentration is more serious and significantly improved when the pillars of the upper and lower coal seams are aligned than when they are staggered. The above studies used numerical simulation methods to extensively introduce the strata movement mechanism in multi-seam mining. However, the numerical simulation results are greatly influenced by the computational models and rock mechanic parameters. In the mining process, if the disturbed computational model and rock mechanic parameters are not adjusted, then the simulation results will not be accepted by other researchers (Adhikary et al. 2015; Ghabraie et al. 2016; Suchowerska et al. 2016; Lin et al. 2013; Khanal et al. 2015).

Some scholars have used physical model experiments to study rock breaking rules in multi-seam mining. Zhang et al. (2015) used a physical model experiment to study the fissure distribution mechanism after three-seam mining. The results showed that the mining width and thickness will jointly affect the developmental height of the fracture zone. The closed fracture zone mainly develops directly above the goaf, while the residual fracture zone is mainly distributed at the start and end of the mining panel. Sui et al. (2014) discussed the influence of the seam interval and thickness of the lower seam on multi-seam mining. The results showed that when $(M, h/M)$ was below an empirical criterion line, multi-seam mining had a large influence on the development of the collapse and fracture zone. Above that empirical line, the caving zone induced by the lower seam will not propagate into the caving zone induced by the upper seam (h is the thickness of the interburden; M is the cutting height of the lower seam). Zhang et al. (2018) study the strata deformation, fracture propagation characteristics and vertical subsidence due to the different extent depending on the multi-seam mining configuration. The results told that multi-seam mining leaded to an enhanced magnitude of subsidence than single-seam mining and the existence of old panel would significantly affects the mechanical response of the newly undermined strata. Tian et al. (2019) used physical model to study the overburden movement with residual pillars. The results showed that the closer to the mining seam, the greater the subsidence of overlying strata. Ghabraie et al. (2015, 2017a, b) arranged goafs with different overlapping

features in the experimental model and studied the surface subsidence and strata movement characteristics above the goaf. The results showed that the strata movement characteristics are different for multi-seam mining as the overlapping features change. Zhu et al. (2018) arranged a multi-seam mining physical model experiment using the room and pillar method. The results showed that a design with some small coal pillars or without any coal pillars can reduce the stress concentration of the upper seam on the lower seam. The research results above illustrated the influence of multi-seam mining on the developmental height and distribution of fissures. However, full mining has never been reached in all physical model experiments mentioned above. Research on the failure process of the interburden and the activation of the upper goaf caused by the failure of the interburden when full mining is reached are limited.

The goal of this paper is to study the failure process of the interburden and the influence of the interburden fracture on the activation of the upper goaf in the process of full longwall multi-seam mining. In this paper, a physical model experiment with two overlapping coal seams is designed. Then, longwall mining is simulated, and the upper coal seam and the lower coal seam are mined in turn to a certain distance to ensure full mining is reached. The displacement and failure process of the rock mass are recorded by Leica-Total Station and photography. Then, the failure process of the interburden and overburden in different locations, the variation in the fracture angle and breaking interval, and the movement mechanism of the subsidence are summarized. The breakage mechanism of the overburden and interburden is analysed. The activation effects of multi-seam mining on the upper goaf left by single-seam mining and the movement mechanism of the surface subsidence are discussed.

2 Physical Modelling of Multi-seam Mining

The physical model experiment must satisfy the principles of similarity theory to ensure that the indoor model can more realistically simulate the real engineering situation. The experiment in this paper is carried out under a self-weight stress field. Therefore, the main similarity constants include the geometric similarity constant C_L and the density similarity constant C_ρ.

$$C_L = L_p/L_m \tag{1}$$

$$C_\rho = \rho_p/\rho_m \tag{2}$$

L_p is the size of the prototype, L_m is the size of the model, ρ_p is the density of the prototype, and ρ_m is the density of the model.

The geometric similarity constant C_L is chosen to be 150 based on the size of the study area and model frame. The density similarity constant C_ρ is selected to be 1.25. Sand-plaster-water mixtures were used to simulate the rock strata. The materials similar to the parameters listed in Table 1 were obtained by adjusting the material ratio. Since the influence of multi-seam mining on strata movement is the sole focus of this study, the strata are simplified into two lithologies, i.e., coal and sandstone, to avoid interference due to a complex combination of strata. Both types of strata have the same material ratio. Moreover, to highlight the appearance of coal seams, ink is used to replace the water that builds in coal seams.

The physical model has the dimensions of 300 cm × 25 cm × 100 cm (length × width × height), which corresponds to an actual engineering scope of 450 m × 37.5 m × 150 m, respectively. In the model, the thickness of the bottom floor and the two coal seams is set to 5 cm, and the thickness of the other stratum is set to 1 cm. The strata were built in sequence from the bottom to the top: (1) the

Table 1 Parameters used in the prototype and model

Name of parameter	Unit	Prototype	Similarity constant	Model
Density	10^3 kg/m^3	2.38	1.25	1.90
Compressive strength	MPa	52.7	187.5	0.281
Elastic modulus	GPa	10.3	187.5	0.055
Cohesion	MPa	8.63	187.5	0.046
Friction angle	°	38.2	1	38.2

bottom floor had a thickness of 5 cm, (2) the lower coal seam had a thickness of 5 cm, (3) the interburden had a total thickness of 15 cm and each stratum had a thickness of 1 cm, (4) the coal seam had a thickness of 5 cm, and (5) the overburden had a total thickness of 70 cm and each stratum had a thickness of 1 cm.

As shown in Fig. 1, the finished model was allowed to air dry for 7 days, and then the total station displacement monitoring lines were set up. A total of nine horizontal monitoring lines were set in this model experiment: seven monitoring lines named 'A' to 'G' in the overburden and two monitoring lines named 'X' and 'Y' in the interburden. In the overburden, the uppermost monitoring line 'A' is 5 cm away from the surface, and the lowest monitoring line 'G' is 5 cm away from the roof of the upper coal seam. The vertical interval of each monitoring line is 10 cm. In the interburden, the monitoring line 'X' is 2.5 cm away from the upper coal seam floor, the monitoring line 'Y' is 2.5 cm from the lower coal seam roof, and the two monitoring lines are also 10 cm apart. The monitoring points on each monitoring line are spaced 10 cm apart in the horizontal direction.

To avoid the influence of the boundary effect of the model frame, the mining range was set to 200 cm long, leaving 50 cm on the left and right sides. Then, a ruler was marked on the model frame, and the coordinate of the start of the mining panel was set to 0 cm, and the end of the mining panel was set to 200 cm. The coal seam was excavated using saw blades, which simulated the actual longwall fully mechanized caving mining method.

Fig. 1 Experimental model after air-drying. (Upper panel indicates the mining range of the upper coal seam. Lower panel indicates the mining range of the lower coal seam. Lines 'A'–'G' represent the seven displacement monitoring lines in the overburden, and Lines 'X' and 'Y' represent the two displacement monitoring lines in the interburden)
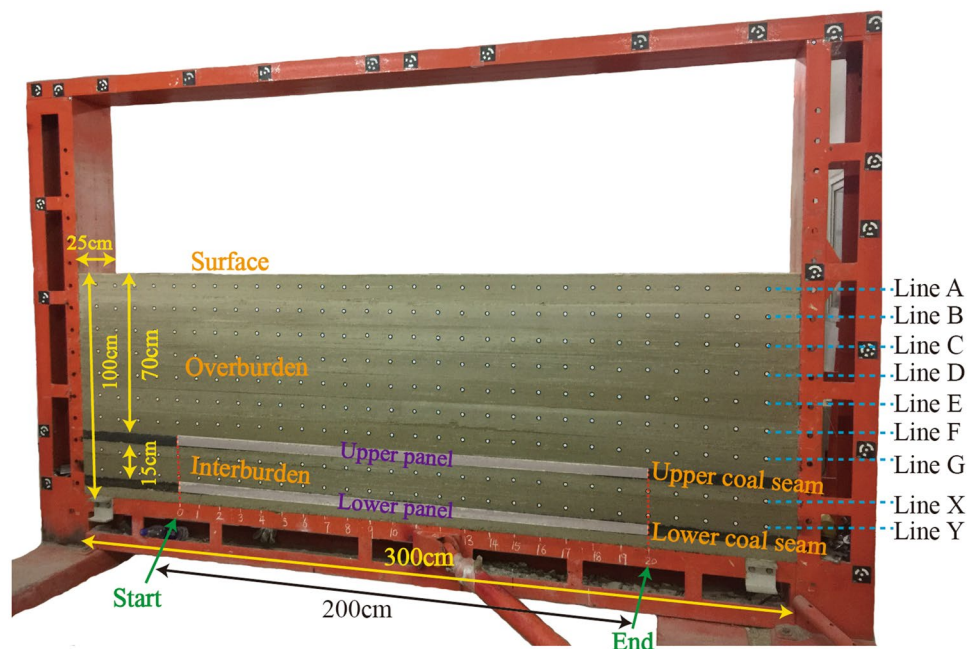
3 Results and Discussion

3.1 Failure Process of Rock Strata

3.1.1 Full Longwall Mining of the Upper Coal Seam

The overburden caved gradually with the mining of the upper coal seam. The first collapse occurred after excavating the upper seam to 67.5 cm (Fig. 2a). The caving rock mass was trapezoidal with 11 strata and was relatively intact in the middle and severely broken on both sides. When the seam was excavated to 92.8 cm, the first periodic weighting
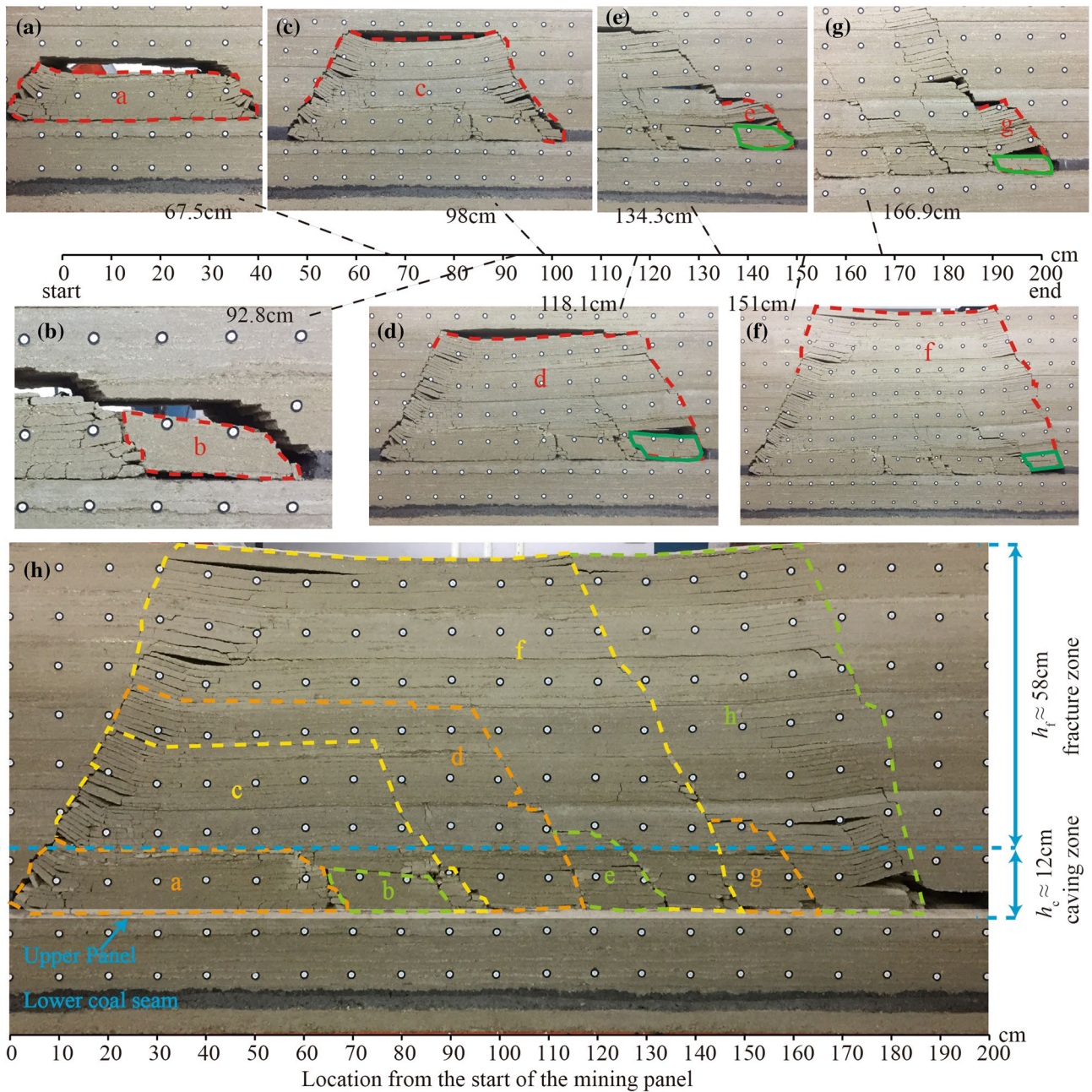
Fig. 2 Appearance of the experimental model while the upper coal seam was being excavated. (The cracks in each collapse are marked with *a–h*. **a–g** Show the current caving status of the rock mass in the mining process. **h** Shows the rock mass collapse pattern after the upper coal seam was mined out. The areas represented by *a–f* in **a–g** are the same as those in **h**. Compared with the status of excavation to 190 cm, the rock mass cracks did not propagate further when the excavation reached 200 cm. Therefore, the current fracture phenomenon of the rock mass when excavated to 190 cm was the same as 200 cm, as shown in **h**. In **d–g**, the green line area indicates the caving zone. h_c and h_f in the figure indicate the height of the caving zone and fracture zone, respectively)

occurred (Fig. 2b), and the morphology of the caving rock mass was quadrilateral and relatively complete and the breaking fissure was in the form of a ladder. When the seam was excavated to 95 cm, a horizontal separation crack approximately 41 cm long appeared at a distance of 37.5 cm from the surface. When it was excavated to 98 cm (Fig. 2c), small-scale collapse occurred at the seam roof, followed by large-scale collapse of the overburden. This result meant that the arch foot of the originally stable arched structure of the overburden was located at the coordinate of 95~98 cm from the start of the mining panel. When the arch foot was destroyed, the original stable structure failed immediately. At this point, the load of the fracture zone was completely applied to the caving zone.

When excavated to 118.1 cm (Fig. 2d) and 134.3 cm (Fig. 2e), the second and third periodic weighting occurred. When excavated to 151 cm (Fig. 2f), the fissure propagated to the surface, and there were two cracks along the vertical mining direction on the surface; the coordinates of the two cracks were 33.4 cm and 114.1 cm. When the height of the fracture reached 12 strata (Fig. 2g), it meshed and connected with the original crack and did not continue to propagate upward. When mining to 190 cm (Fig. 2h), the surface broke again, and a new fissure appeared along the mining direction. After excavating to the end of the mining panel, the rock mass was suspended to form a stable cantilever beam structure in which a collapse did not occur.

After the upper coal seam was mined out, it was observed that the contact parts of the caving zone adjacent to the two collapses became more fractured than other parts due to the disturbance of tilting and compaction.

As shown in Fig. 3, the load distribution of the surrounding rock in single-seam mining can be divided into four stages. In the first stage, the overburden strata can always form a stable arch-shaped support structure after each collapse. The surrounding rock load is all applied on the stable structure. In the second stage, fissures propagate to the surface, and the surrounding rock load squeezes into the goaf. The horizontal loads cancel each other in the fracture zone, which leaves only the vertical stress applied on the caving zone. During the third stage, as the mining moves forward, the caving zone continues to move forward while the stable structure of the previous stage remains unchanged. In the fourth stage, after a certain distance is mined, the stable structure is destroyed again, and the fracture zone moves forward. The load distribution in the fourth stage is similar to that in the second stage. Subsequently, as the mining continues, the third and fourth stages alternate.

After mining, according to the shape of the goaf and load distribution, the surrounding rock can be divided into 'Z1'–'Z4', the fracture zone into 'M1'–'M3', and the caving zone into 'N1'–'N3' (Fig. 4 left). 'Z1' and 'Z2' squeeze into the goaf, resulting in the squeezing load F. 'M2' and 'M3' transfer the load F onto 'M1'. 'M1' balances itself
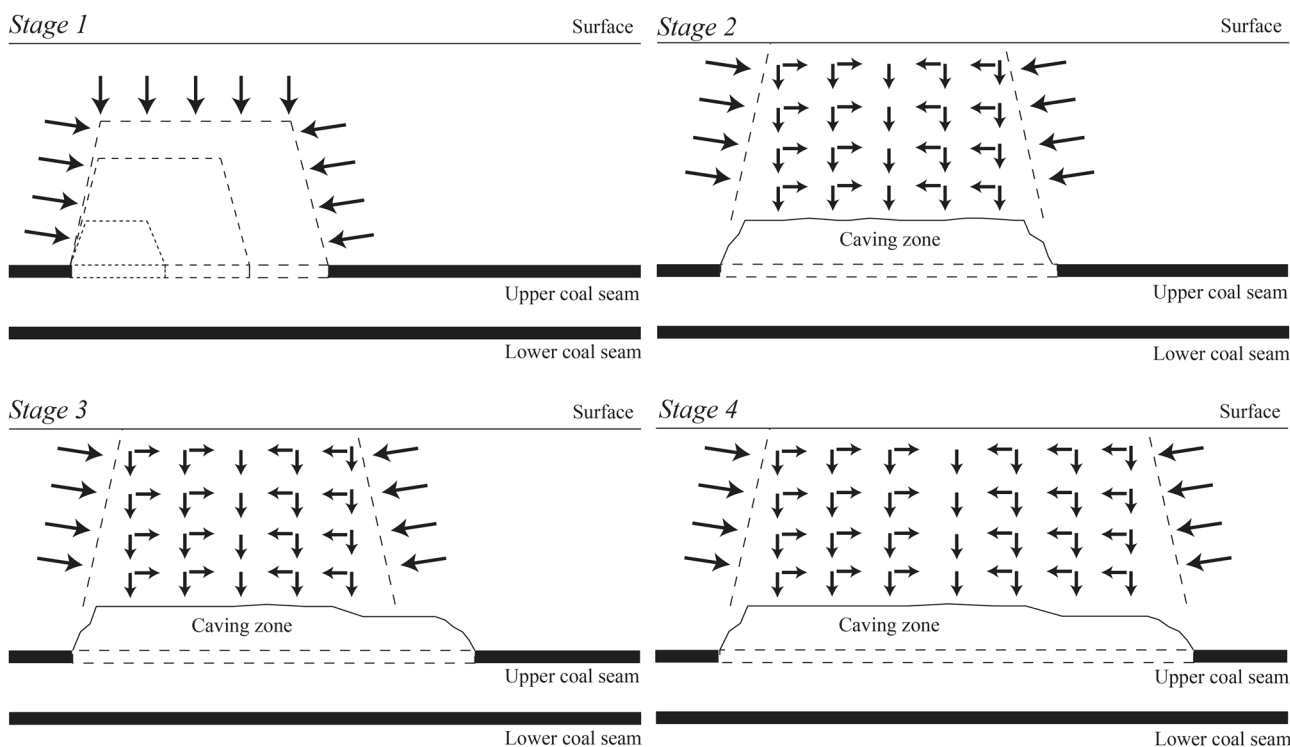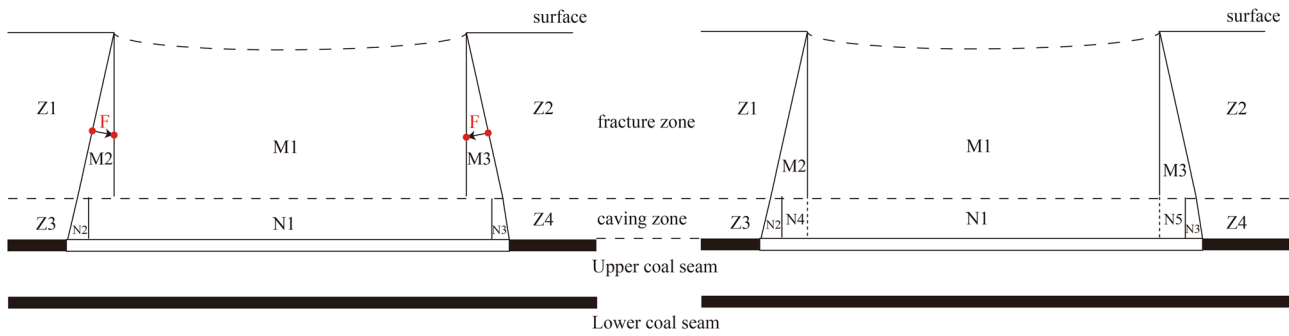

Fig. 3 Schematic diagram of the four stages of dynamic load changes when the upper seam is mined

Fig. 4 Schematic diagram of the surrounding rock division after the upper coal is mined out

horizontally and then transfers the load and its own weight downward to 'N1'. 'N2' and 'N3' are the caved areas that are not filled, which are close to the start and end of the mining panel and do not bear any load. However, zones 'Z3' and 'Z4' are areas of increasing load because they are subjected to a compressive load that is greater than before mining began.

Since the force locations of the 'M2' area are also on 'Z1' and 'M1', respectively (the red points on the left side of Fig. 4), no load influence is generated downward. Therefore, we can separate the 'N4' region from the 'N1' region (right side of Fig. 4), which does not bear the load from the overburden, and the load on the rock mass below is only the self-weight of the caving rock mass here, which is the region of decreasing load. Similarly, the 'N5' area can be separated out at the end of the mining panel (right side of Fig. 4). After the upper coal seam is mined out, the load distribution of the overburden on the interburden is shown in Fig. 5. Because

the load in the 'Z3' and 'Z4' regions has little influence on the interburden, the focus is the overburden load in the goaf. In particular, the load in the 'N1' area needs to consider the influence of the distribution form of each periodic weighting. We plotted the load q_1 block in Fig. 5.

3.1.2 Full Longwall Mining of the Lower Coal Seam

Figure 6 shows the rock mass collapsed status in the lower coal seam mining. When the lower coal seam was excavated to 53.5 cm (Fig. 6a), the whole interburden collapsed, and the lower goaf was directly connected with the upper goaf. The breaking fissure above the working face not only cut through the interburden completely but also propagated upward and cut the fractured rock mass in the goaf of the upper coal seam, which resulted in a more broken rock mass. When mined to 63.3 cm (Fig. 6b), the longitudinal cracks in the previously collapsed rock mass widened, lengthened, and
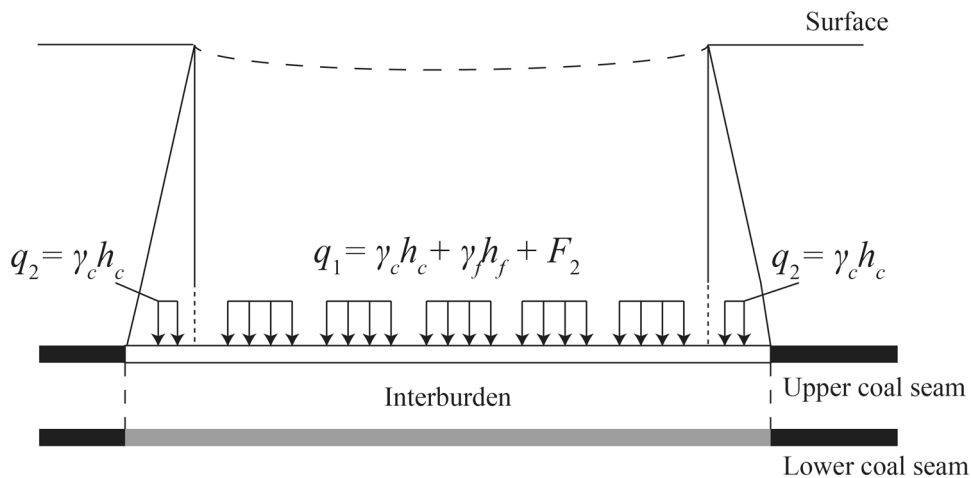
Fig. 5 Schematic diagram of the distribution of the overlying load on the interburden after the upper coal seam is mined out. (γ_c and γ_f in the figure indicate the unit weight of the caving zone and fracture zone, respectively. h_c and h_f in the figure indicate the height of the caving zone and fracture zone, respectively. 'F2' represent the verti-

cal component of the squeezing pressure of the surrounding rock mass toward the goaf. The load q_1 block is drawn to indicate the load on the interburden of the collapsed rock mass in each periodic weighting.)
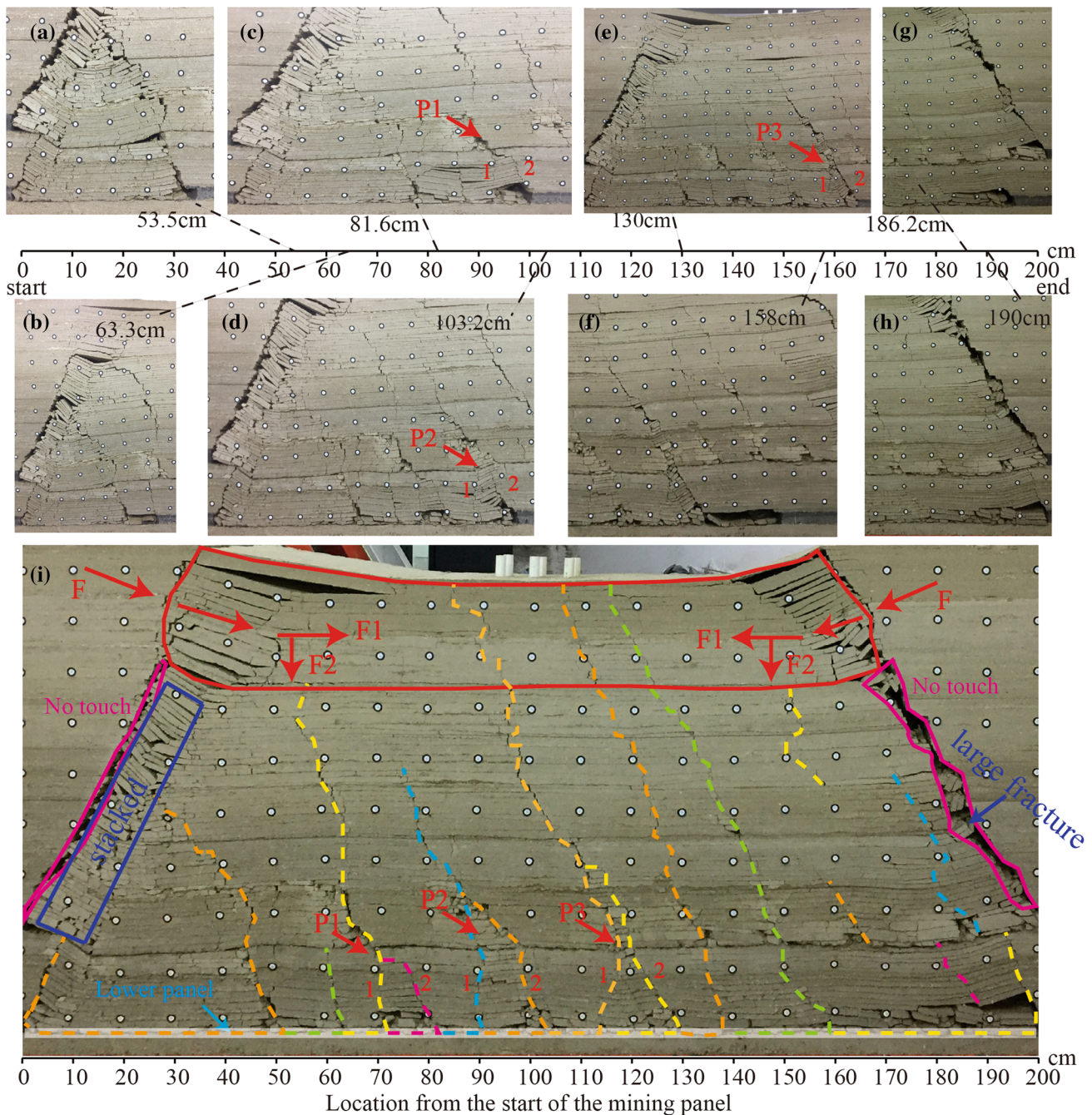
Fig. 6 Appearance of the experimental model while the lower coal seam was being excavated. ('P1', 'P2' and 'P3' in Figs. 3, 4 and 5) correspond to 'P1', 'P2' and 'P3' in Fig. 9, respectively. 'F' represents the squeezing pressure of the surrounding rock mass towards the goaf. 'F1' and 'F2's represent the horizontal and vertical component of 'F', respectively)

penetrated through the interburden. At the same time, the cracks propagated upward, and the caving zone and fracture zone above the goaf of the upper coal seam were sheared repeatedly. When mining the lower seam to 73.2 cm, another longitudinal crack appeared above the working face; at this time, the rock mass showed obvious bending failure. When it was excavated to 81.6 cm (Fig. 6c), the rock body that

was damaged by previous bending fell onto the floor. As the mining progressed, the failure of the rock mass showed the process of 'breaking'—'bending'—'crack propagation'—'falling onto the floor' (Fig. 6b–f). At the location close to the end of the mining panel (Fig. 6g–i), the interburden showed an obvious cantilever beam bending failure process, and the breaking interval was long. After mining the lower

coal seam, the load on the fracture zone generated by the upper coal mining was unloaded, resulting that the strata above the start of the mining panel were stacked and a large fracture occurred above the end of the mining panel.

The first collapse that was caused by a sudden compression-shear failure under the self-weight of the overburden, and the subsequent failure was a bending failure of the plate. The cracks in the interburden basically developed near the contact position of the caving zone during the periodic weighting in the upper coal seam mining, and more than one downward extending crack developed at each contact position. As shown in Fig. 6, six cracks in total developed downward at points 'P1', 'P2' and 'P3'. Cracks #1 and #2 that developed at point 'P1' formed a trapezoid with a short upper bottom and a long lower bottom, and cracks at points 'P2' and 'P3' did also. Interestingly, crack #2 that developed at point 'P1' and crack #1 that developed at point 'P2' cut the interburden into a trapezoid with a long upper bottom and a short lower bottom. Thus, crack #2 developed at point 'P2', and crack #1 developed at point 'P3' did also. This phenomenon occurred only near the central part of the goaf. Therefore, we inferred that the uneven load of the periodic weighting fragments in the upper goaf resulted in a breaking morphology of trapezoid interlocking.

After the upper coal seam was mined out, the height of the caving zone was approximately 11 cm above the goaf, while the other parts were all fracture zones bearing the squeezing pressure caused by the surrounding rock mass that rushed into the goaf. After the lower coal seam was mined out, the rock mass as a whole subsided, and the load on the fractured rock mass at the location of the start of the mining panel and the end of the mining panel was unloaded. Therefore, a part of the fracture zone that formed by mining the upper coal seam would be converted into the caving zone and no longer bear the squeezing pressure from the surrounding rock. The original squeezing pressure was transferred into the remaining fracture zone (Fig. 6i).

As shown in Fig. 7, when the lower coal seam is mined out, fissures gradually appear as the mining distance increases. Because the load q_2 near the start of the upper mining panel is small, the failure of the interburden will not occur in a short mining distance. When mining to a certain distance, the first failure of the interburden is the shear failure of the simply supported beam due to the increased load q_1 (Fig. 7-1). As the mining continues, the fissures propagate downward at the contact position between the first caving and the second caving in the upper coal seam (Fig. 7-2). Since the interburden is thin and the upper load is large, after mining a certain distance, the interburden exhibits cantilever beam bending failure. Moreover, due to the influence of the periodic weighting interval during upper seam mining, the fissures in the interburden always propagate downward from the contact position of the adjacent caving zones in

the upper coal seam, which results in a smaller breaking interval of the interburden. However, at the location close to the end of the mining panel, the interburden is subjected to a smaller load q_2 from the overburden, which leads to a larger breaking interval.

When the lower coal seam is mined out, the 'M1' region will move downward (left side of Fig. 8), resulting in the disappearance of the force application points in the 'M2' and 'M3 regions and the unloading (red point in Fig. 4). Due to the large number of separation cracks in the 'M2' region after upper coal seam mining, the rock mass in that area is stacked after unloading due to mining the lower coal seam. However, in the 'M3' region, there are fewer separation cracks when the upper coal seam is mined out, and they are mainly tensile fractures. During this unloading process, the tensile cracks will expand to form larger fractures. This phenomenon indicates that most of the fracture zone is transformed into a caving zone. The load division after mining the lower coal seam is shown on the right side of Fig. 8. This process is the activation effect on the upper goaf that was left by mining the upper coal seam when the lower coal seam is being mined out.
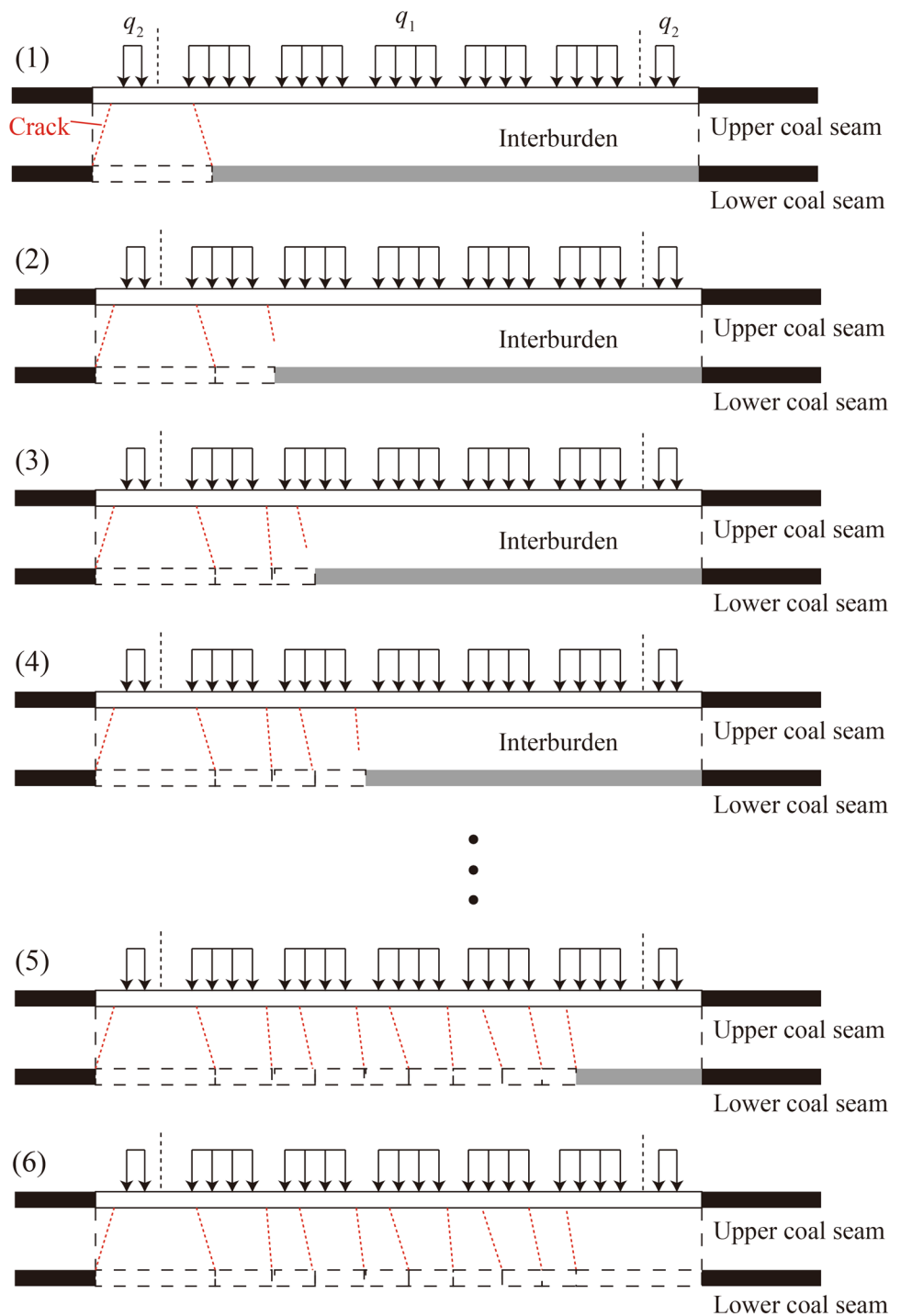
3.2 Breaking Interval

As shown in the rock mass failure process in Sect. 3.1, there was an obvious periodic weighting phenomenon when the upper coal seam was mined. Therefore, the first collapse and the periodic weighting in upper seam mining were defined as 'breaking interval'.

However, when the lower coal seam was mined, the failure of the interburden showed obvious plate bending failure, except for the first collapse. The process of roof collapse to the floor was slow, and there was no obvious periodic weighting phenomenon in the failure process. Therefore, we defined the interval between two neighbouring and penetrating cracks in the interburden as 'breaking interval', when the lower seam was mined.

As shown in Fig. 9, when the upper coal seam was mined out, the first collapse interval was large (67.5 cm), but then the first interval decreased rapidly (25.3 cm). The second interval was similar to that of the first interval and then decreased. In the following three intervals, the interval remained at the same level (approximately 16 cm). The last interval slightly increased (23.1 cm). Although the periodic weighting intervals varied slightly, they generally remained at a similar level (16–25 cm).

When the lower coal seam was mined out, the first breaking interval was smaller than that of the upper coal seam. Subsequently, the breaking interval of the interburden was smaller than that of the overburden when the upper coal seam was mined out, which was approximately 10–15 cm.

Fig. 7 Schematic diagram of the breakage of the interburden when the lower coal seam is mined out


At a location close to the end of the mining panel, the breaking interval gradually increased.

3.3 Angle of Fracture

The angle of fracture includes the angle of left-fracture named α and the angle of right-fracture named β in Fig. 10. The angle of left-fracture is defined as the angle between the fissure and the horizontal plane extending to the right at the start of the mining panel, and the angle of right-fracture is defined as the angle between the fissure and the horizontal plane extending to the left at other locations.

When the upper seam was mined out, the angle of left-fracture was 54° ($\alpha1$) during the first collapse. During the mining process, cracks propagated to the surface, and the angle of left-fracture increased from $\alpha1$ to $\alpha4$. After
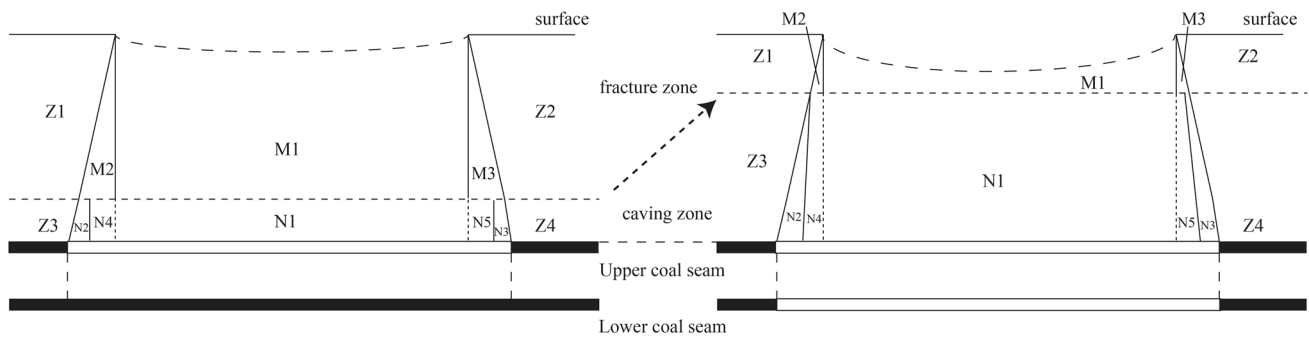
Fig. 8 Schematic diagram of the load division after mining the upper (left) and lower (right) coal seams

the upper seam was mined, the angle of left-fracture was approximately 76° (α4). When the lower seam was mined, the angle of left-fracture was 66° (α5) during the first collapse. As the mining advanced, the angle of left-fracture remained unchanged because of the direct penetration of the interburden between two goafs during the first collapse.

Figure 11 shows the variation in the angle of right-fracture in the mining process. When the upper coal seam was mined, the angle of right-fracture increased or decreased, but the overall trend was an increasing angle. When the lower coal seam was mined, the angle of right-fracture first showed an upward trend and then a downward trend. Notably, in the process of coal seam mining (from left to right), the overburden collapsed and squeezed into the mined out area, which also caused the compression-shear failure in start location and tensile shear failure in end location. Therefore, whether it was single-seam or multi-seam mining, the angle of right-fracture close to the start of the mining panel was larger than that close to the end of the mining panel (α4 < β7, α5 < β18 in Fig. 10). Besides, because the coal height of multi-seam was larger than single-seam, the tensile shear failure was more serious after lower seam was mined out. The angle of right-fracture of the interburden was larger than that of the overburden (β7 < β18 in Fig. 10).
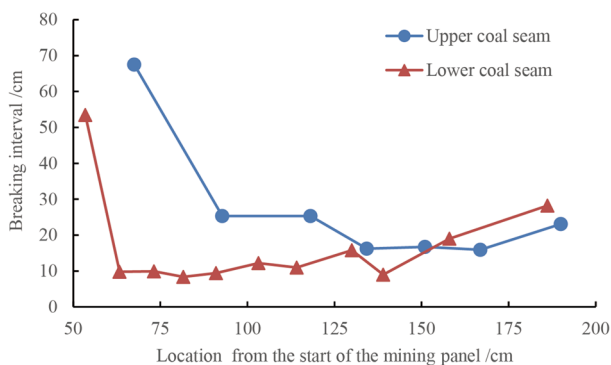
Fig. 9 Breaking interval when the two coal seams were mined

3.4 Subsidence

Figure 12 is the subsidence curve of each monitoring line when the upper coal seam was mined out. Line 'A' is the monitoring line, 5 cm away from the surface, used to represent the subsidence characteristics of the surface. From Fig. 12a, there were obvious troughs in the subsidence of all monitoring lines, indicating that the upper seam had been fully mined. The closer the monitoring line was away from the coal seam, the wider the subsidence trough and the steeper the trough margin were. For example, the subsidence trough of Line G was wider and steeper than Line A–F. This is because the rock mass close to the coal seam is seriously damaged and swells, which has a buffer effect on the subsidence of the rock mass far away from the coal seam. Although each monitoring line obviously showed trough characteristics, the trough bottom was not horizontal, and the subsidence near the start of the mining panel was larger. The subsidence curves all exhibited features that inclined toward the start of the mining panel. In addition, the subsidence trough of lines 'F' and 'G' (close to the roof) were not as flat as other monitoring lines. This effect was due to the movement of the rock mass during the process of the roof collapse, such as inclination and stacking, which led to uncoordinated subsidence.

Figure 12b shows the subsidence of the monitoring line in the lower coal seam mining. A clear trough appeared on line 'A', which was near the surface, indicating that the lower coal seam had been fully mined. The location of the subsidence curve near the trough margin was steeper than that of the upper coal seam mining, which indicated that multi-seam mining would cause a larger subsidence difference around the trough margin area. However, the width of the trough did not change. At the same time, the uncoordinated subsidence of the rock mass over the goaf during the upper coal mining also appeared in lines 'X' and 'Y'. However, we also observed that the uncoordinated subsidence of lines 'F' and 'G' weakened, which indicated
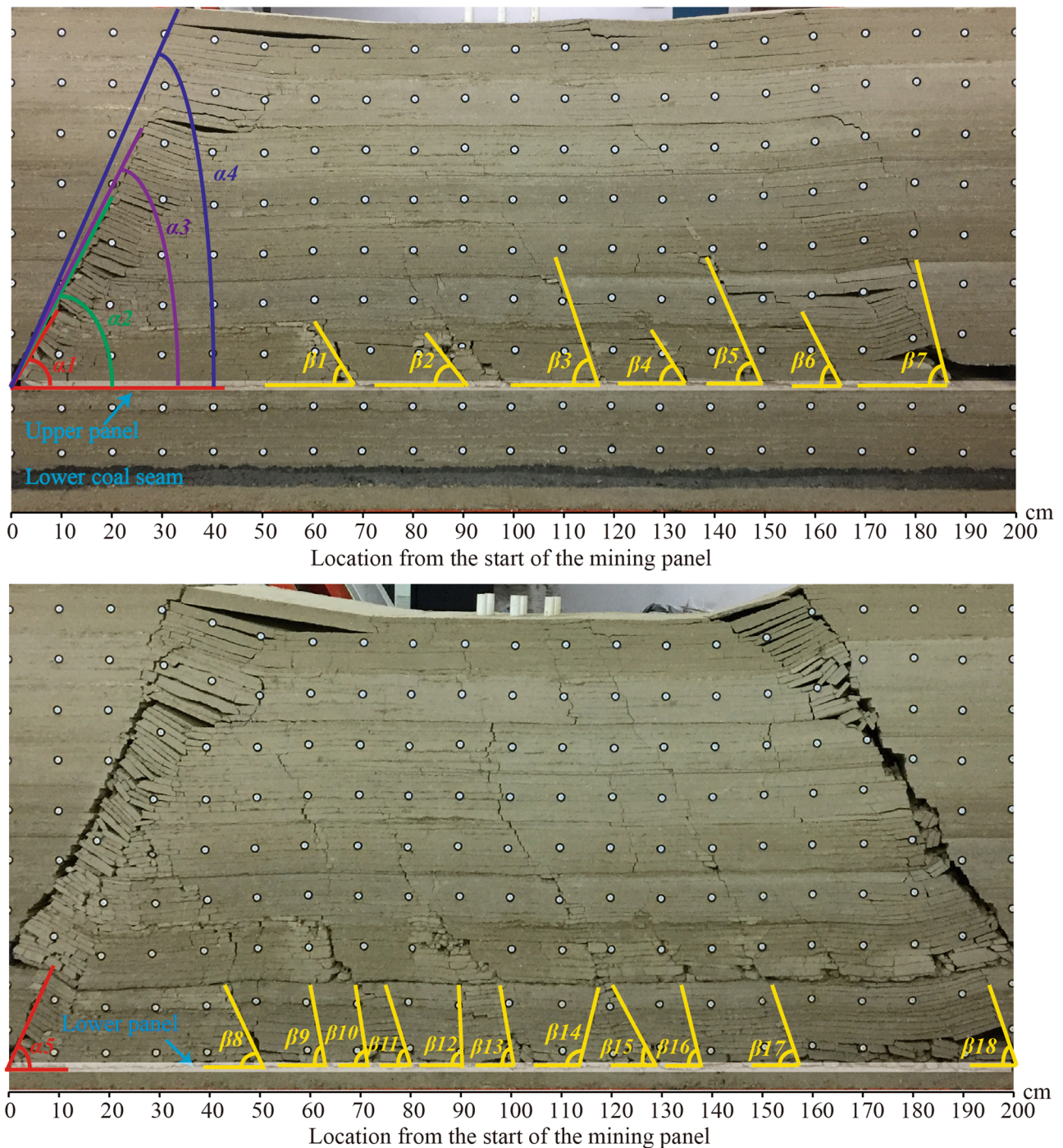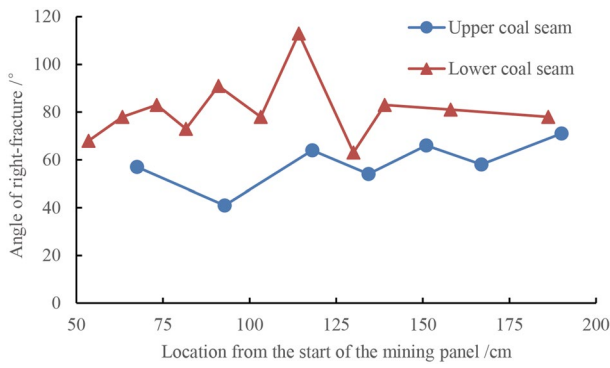
Fig. 10 Angle of fracture when the two coal seams were mined

that multi-seam mining would cause the rock mass in the upper goaf to re-adjust its position and settle uniformly.

In Fig. 12b, after the lower coal seam mining, the monitoring lines 'E' 'F' and 'G' exhibited similar characteristics to the subsidence curve of single-seam mining (Fig. 12a). That is, the subsidence above the start of the mining panel was the largest and decreased rapidly as the distance from a location increased. However, in addition to the three lines mentioned above, lines 'A'–'D' showed inclinations toward the start of the mining panel in Fig. 12a, but they changed to incline toward the end of the mining panel in Fig. 12b. As shown in Fig. 13, the subsidence curve of line 'A' showed an obvious inclination to the start of the mining panel in single-seam mining (the legends 'Upper-151.0'

Fig. 11 Angle of right-fracture when the two coal seams were mined

and 'Upper-200.0'). With the mining process of the upper coal seam, the subsidence trough gradually moved toward the centre of the goaf. However, during the mining process of the lower coal seam, the trough widened slightly

(legends 'Lower-40.0′'–'Lower-73.2'), and then the subsidence increased suddenly (legend 'Lower-103.2'). With the mining of the lower coal seam, the subsidence trough gradually transferred toward the end of the mining panel (legend 'Lower-200.0'), and the subsidence curve inclined greatly at the end of the mining panel.

We defined the subsidence factor F_s as follows:

$$F_s = S_{surface}/M \tag{3}$$

$S_{surface}$ means the maximal subsidence of surface and M means the total mining height of coal.

After the upper coal seam was mined out, the maximum subsidence of the surface was 2.9 cm, and the average subsidence was 2.6 cm. Thus, the maximum subsidence factor was 0.58 and the average was 0.52. After the lower coal seam was mined out, the maximum subsidence was 7.4 cm and the average subsidence was 7.1 cm. Therefore, the maximum subsidence factor was 0.74 and the average was 0.71.
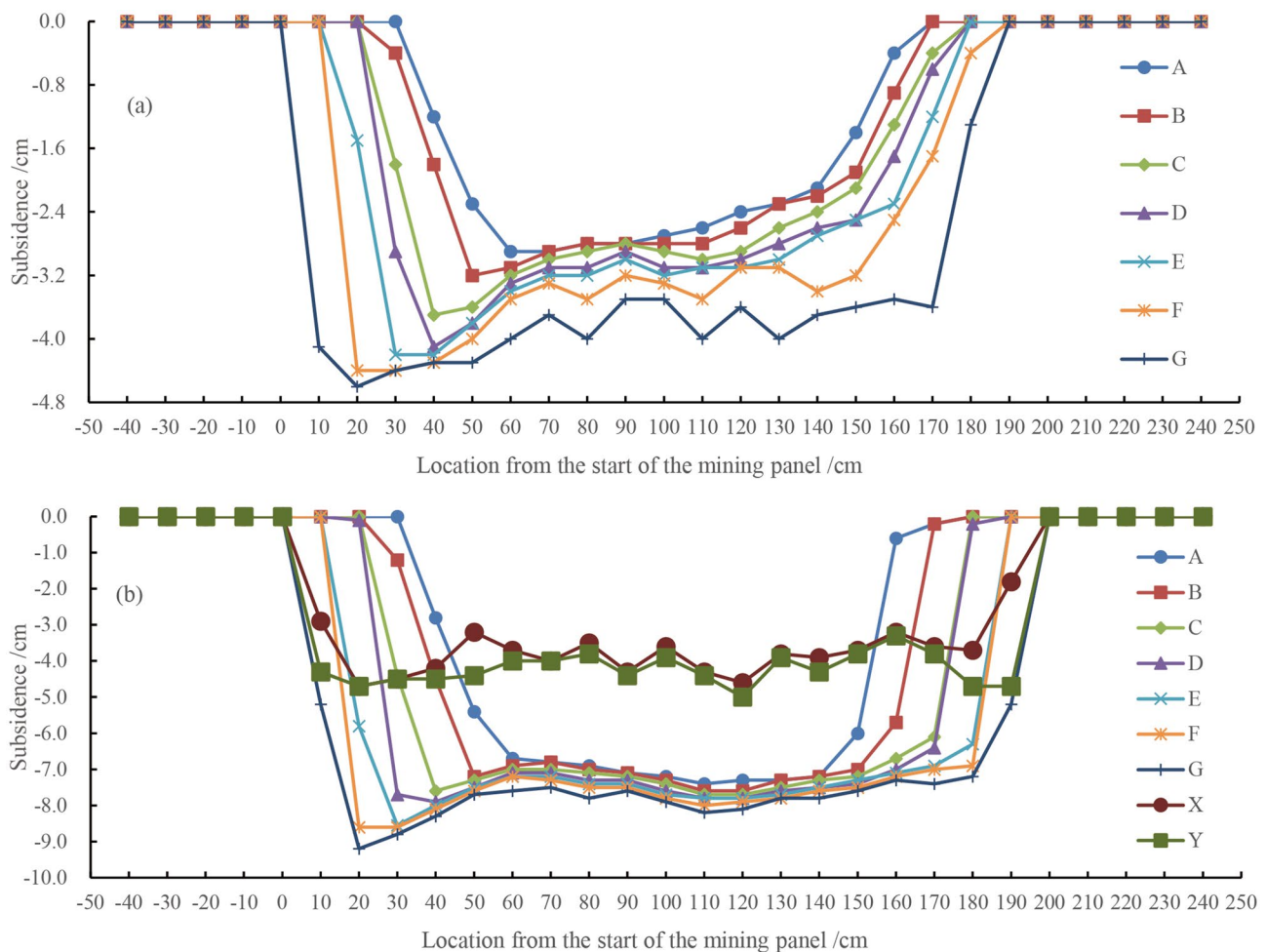
Fig. 12 **a** Subsidence of the monitoring lines after the upper coal seam was excavated. **b** Subsidence of the monitoring lines after the lower coal seam was excavated. (The legends 'A'–'G' in this figure are same as in Fig. 1)
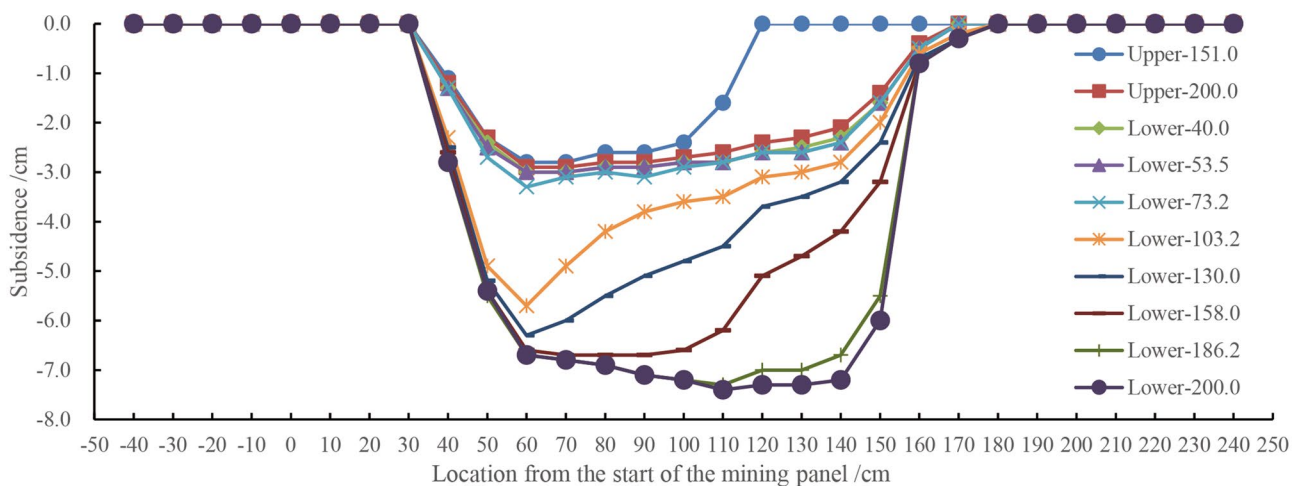
Fig. 13 Subsidence of the monitoring line 'A' during different processes of excavation. (The legends in this figure stand for the upper or lower coal seam and the distance of the excavation)

This phenomenon showed that multi-seam mining would greatly increase the subsidence factor.

During the process of mining the upper coal seam, rock failure near the goaf is mainly caused by caving. The closer the stratum is to the start of the mining panel, the weaker the bloating-breaking effect is. Therefore, after the upper coal seam is mined, the subsidence of the upper rock strata tends toward the start of the mining panel. While in lower coal seam mining, since the rock mass has been inclined to the start of the mining panel, the rock mass close to the end of the mining panel will not be crushed and stacked but will be layered. In particular, there may even be a phenomenon of filling residual voids near the end of the mining panel. Therefore, the rock near the end of the mining panel has a better compaction effect, the subsidence is larger, and the subsidence curve is steeper. Especially after the effect is transferred to the surface, the phenomenon that the trough moves toward the end of the mining panel is more obvious.

4 Conclusions

With the depletion of near-surface coal resources, multi-seam mining engineering has attracted increasing attention. However, the mechanism of rock breakage and activation of the upper goaf have not yet been fully described for mining under an upper goaf. To deepen our understanding of this issue, we use a physical model experiment to study the rock strata movement of multi-seam mining in overlapping double seams that are all fully mined. The regularity of the interburden breakage caused by multi-seam mining and the mechanism of deformation and activation of the fractured rock mass in an overlying upper goaf are analysed. The main conclusions are as follows:

1. During the mining process of the lower coal seam, the interburden at the start of the mining panel exhibits shear failure, and other locations are characterized by bending failure of the plate.

2. The contact position of the caving zone generated by the periodic weighting of the upper seam mining affects the load distribution of the interburden and controls the break interval, which causes the break interval to be larger near the start and end of the mining panel. Then, the interval becomes small in the centre of the goaf. The breakage of the interburden is influenced by this rule, and the morphology of the caving rock mass presents a stacking trapezoid. At the same time, the fracture of the interburden will re-activate the mining-induced fracture in the overburden and increase the developmental height and width of the fracture.

3. Multi-seam mining will transform the fracture zone produced by single-seam mining into a caving zone within a certain height range and cause the residual fracture zone above to bear a greater compressive load. The unloaded rock mass near the start of the mining panel will be stacked in layers, while the rock mass close to the end of the mining panel will directly break to form a wide fracture.

4. In full single-seam mining, the surface subsidence trough is offset to the start of the mining panel. However, the surface settlement in full multi-seam mining will be shifted to the end of the mining panel. The subsidence near the end of the mining panel is larger than that close to the start of the mining panel. Multi-seam mining will re-adjust the location of the uncoordinated deformation rock mass generated by caving the old roof during single-seam mining, which makes the subsidence more uniform.

References

Adhikary D, Khanal M, Jayasundara C, Balusu R (2015) Deficiencies in 2D simulation: a comparative study of 2D versus 3D simulation of multi-seam longwall mining. Rock Mech Rock Eng 49(6):2181–2185

Ghabraie B, Ren G, Zhang X, Smith J (2015) Physical modelling of subsidence from sequential extraction of partially overlapping longwall panels and study of substrata movement characteristics. Int J Coal Geol 140:71–83

Ghabraie B, Ghabraie K, Ren G, Smith JV (2016) Numerical modelling of multistage caving processes: insights from multi-seam longwall mining-induced subsidence. Int J Numer Anal Met 41(7):959–975

Ghabraie B, Ren G, Smith JV (2017a) Characterising the multi-seam subsidence due to varying mining configuration, insights from physical modelling. Int J Rock Mech Min 93:269–279

Ghabraie B, Ren G, Barbato J, Smith JV (2017b) A predictive methodology for multi-seam mining induced subsidence. Int J Rock Mech Min 93:280–294

Helm PR, Davie CT, Glendinning S (2013) Numerical modelling of shallow abandoned mine working subsidence affecting transport infrastructure. Eng Geol 154:6–19

Iwanec AMS, Carter JP, Hambleton JP (2016) Geomechanics of subsidence above single and multi-seam coal mining. J Rock Mech Geotech Eng 8(3):304–313

Khanal M, Adhikary D, Jayasundara C, Balusu R (2015) Numerical study of mine site specific multiseam mining and its impact on surface subsidence and chain pillar stress. Geotech Geol Eng 34(1):217–235

Lin N, Sasaoka T, Shimada H, Hamanaka A, Matsuia K (2013) Numerical analysis of interaction effects in double extra-thick coal seams mining. Proc Earth Planet Sci 6:343–349

Liu X, Tan Y, Ning J, Tian C, Wang J (2015) The height of water-conducting fractured zones in longwall mining of shallow coal seams. Geotech Geol Eng 33(3):693–700

Ma WJ, Hu HF (2013) The strata movement regularity and parameter simulation analysis in multiple seams repeated mining. Appl Mech Mater 295–298:2935–2939

Ma WM, Zhu WY (1984) Effect of multi-seam mining on subsidence. Int J Min Eng 2(2):171–173

Miao X, Cui X, Wang JA, Xu J (2011) The height of fractured water-conducting zone in undermined rock strata. Eng Geol 120(1–4):32–39

Porathur JL, Srikrishnan S, Verma CP, Jhanwar JC, Pal Roy P (2014) Slope stability assessment approach for multiple seams highwall mining extractions. Int J Rock Mech Min 70:444–449

Ren G, Li G, Kulessa M (2014) Application of a generalised influence function method for subsidence prediction in multi-seam longwall extraction. Geotech Geol Eng 32(4):1123–1131

Salmi EF, Nazem M, Karakus M (2017) Numerical analysis of a large landslide induced by coal mining subsidence. Eng Geol 217:141–152

Suchowerska AM, Merifield RS, Carter JP, Clausen J (2012) Prediction of underground cavity roof collapse using the Hoek-Brown failure criterion. Comput Geotech 44:93–103

Suchowerska AM, Merifield RS, Carter JP (2013) Vertical stress changes in multi-seam mining under supercritical longwall panels. Int J Rock Mech Min 61:306–320

Sui W, Hang Y, Ma L, Wu Z, Zhou Y, Long G, Wei L (2014) Interactions of overburden failure zones due to multiple-seam mining using longwall caving. B Eng Geol Environ 74(3):1019–1035

Tang CA, Yang WT, Fu YF, Xu XH (1998) A new approach to numerical method of modelling geological processes and rock engineering problems—continuum to discontinuum and linearity to nonlinearity. Eng Geol 49(3–4):207–214

Tian C, Yang X, Sun H, Liu Y, Hu Q (2019) Experimental study on the overburden movement and stress evolution in multi-seam mining with residual pillars. Energy Sci Eng 7(6):3095–3110

Tulu IB, Esterhuizen GS, Klemetti T, Murphy MM, Sumner J, Sloan M (2016) A case study of multi-seam coal mine entry stability analysis with strength reduction method. Int J Min Sci Technol 26(2):193–198

Wang DC, Yang YJ, Wang K, Zhao NN (2012) Numerical simulation of study on rupture development rules of overburden strata in repeated mining. Adv Mat Res 433–440:1933–1939

Wang G, Wu M, Wang R, Xu H, Song X (2017) Height of the mining-induced fractured zone above a coal face. Eng Geol 216:140–152

Wei X-Q, Bai H-B, Rong H-R, Jiao Y, Zhang B-Y (2011) Research on mining fracture of overburden in close distance multi-seam. Proc Earth Planet Sci 2:20–27

Ying-ke L, Fu-bao Z, Lang L, Chun L, Shen-yong H (2011) An experimental and numerical investigation on the deformation of overlying coal seams above double-seam extraction for controlling coal mine methane emissions. Int J Coal Geol 87(2):139–149

Zhang Y, Yan L (2015) Experimental study on distribution law of residual fissure under multiple mining conditions. Revista de la Construcción J Constr 14(1):77–81

Zhang M, Shimada H, Sasaoka T, Matsui K, Dou L (2013) Evolution and effect of the stress concentration and rock failure in the deep multi-seam coal mining. Environ Earth Sci 72(3):629–643

Zhang X, Ghabraie B, Ren G, Tu M (2018) Strata movement and fracture propagation characteristics due to sequential extraction of multiseam longwall panels. Adv Civil Eng. https://doi.org/10.1155/2018/4802075

Zhu D, Tu S (2017) Mechanisms of support failure induced by repeated mining under gobs created by two-seam room mining and prevention measures. Eng Fail Anal 82:161–178

Zhu Z, Zhang H, Nemcik J, Lan T, Han J, Chen Y (2018) Overburden movement characteristics of top-coal caving mining in multi-seam areas. Q J Eng Geol Hydrogeol 51(2):276–286